An Electron Cyclotron Resonance Plasma Configuration for Increasing the Efficiency in the Yield of Nitrogen Endohedral Fullerenes

An electron cyclotron resonance plasma configuration for increasing the efficiency in the yield of nitrogen endohedral fullerenes

T. Kaneko, S. Abe, H. Ishida, and R. Hatakeyama
Department of Electronic Engineering, Tohoku University, Sendai, 980-8579, Japan

(Received 17 August 2007; accepted 29 October 2007; published online 28 November 2007)

Efficiently yielding a nitrogen-atom endohedral fullerene ($N@C_{60}$) is demonstrated for the first time using an electron cyclotron resonance (ECR) plasma source with a minimum-B mirror configuration realized by hexapole permanent magnets. Since electrons are effectively confined around a bottom of the minimum-B mirror in the ECR region, the high-temperature electrons can be generated there, and as a result, the dissociation degree of the nitrogen molecules increases drastically. This highly dissociated nitrogen plasma has a number of nitrogen-atom radicals and ions, thus permitting an enhancement of $N@C_{60}$ yield. © *2007 American Institute of Physics*. [DOI: 10.1063/1.2814049]

The insertion of various kinds of atoms or molecules into the cage of fullerenes, i.e., the formation of metal or gas endohedral fullerenes, has been actively investigated because of their unique structural and electric/magnetic/optical properties. Recently, a nitrogen-atom endohedral fullerene ($N@C_{60}$) has attracted considerable interest as a candidate for quantum computing devices that will constitute electronic systems alternative to silicon-ruled semiconductor ones.[1] ($N@C_{60}$) has been yielded by ion implantation,[2] glow discharge,[3,4] and radio frequency discharge[5,6] methods so far, where C_{60} films deposited on substrates are exposed continuously to nitrogen ions accelerated by electric fields actively or passively. However, the synthesis yield of $N@C_{60}$ is extremely low (purity just after the synthesis: $N@C_{60}/C_{60}=10^{-3}\%-10^{-2}\%$) at present. Although the purity can be improved by high performance liquid chromatography (HPLC),[7–9] HPLC takes an awfully long time to purify the extremely low yield of $N@C_{60}$. Therefore, the synthesis of $N@C_{60}$ with high yield is essential to obtain the high-purity and finally isolated $N@C_{60}$ for investigating the promising properties of $N@C_{60}$.

The synthesis of $N@C_{60}$ requires a plasma containing a considerable amount of nitrogen-atom radicals N^* and/or ions N^+ as an encapsulated source of nitrogen atom. To produce N^* and N^+ from nitrogen molecules N_2 ($N_2+e\rightarrow N^*+N^++2e$), a desorption/ionization energy of 25.4 eV should be supplied to N_2 by energy transfer from electrons.[10] In this respect, an electron cyclotron resonance (ECR) discharge in a mirror magnetic field is useful, which leads to the energization of the electrons and the resultant dissociation and ionization of N_2.[11] Furthermore, the electrons are expected to be effectively confined by the radially increased magnetic field generated by hexapole permanent magnets, which is superimposed on the conventional axial mirror magnetic field.[12,13] This axially and radially increased magnetic field is defined as a minimum-B mirror configuration, and is effective for the synthesis of $N@C_{60}$.[14]

In this letter, the efficient synthesis of $N@C_{60}$ is demonstrated by actively controlling the plasma parameters such as plasma density, electron temperature, and ion species using the ECR plasma source with the minimum-B mirror configuration.

The experimental setup is schematically shown in Fig. 1, where a microwave is launched into a stainless steel chamber of 11 cm diameter through a waveguide by a microwave generator (2.45 GHz, 800 W). N_2 is fed into the chamber and ionized under the influence of the microwave. The plasma is divided into two regions, i.e., the ECR and process regions, using a separation grid supplied with a negative voltage V_g. Solenoid coils surrounding the chamber generate inhomogeneous magnetic fields, which form mirror configurations in the ECR region and diverge slightly in the process region. The axial profile of the magnetic field at the radial center is calculated and shown in the bottom figure in Fig. 1. The hexapole neodymium permanent magnets for radial confinement of the plasma are mounted around the bottom of the axial mirror magnetic field, and the minimum-B mirror configuration is realized in the ECR region. Here, the profile of conventional axial mirror magnetic field is defined as a simple mirror (SM) configuration and is distinguished from the minimum-B mirror (MM) configuration.

Since electrons in the ECR region are trapped in the mirror magnetic field and accelerated owing to ECR at the bottom of the mirror configuration (875 G), a number of N^* and N^+ are expected to be produced as a result of the effective dissociation and ionization of N_2 gas. The ECR plasma containing the nitrogen ions diffuses toward the process region through the separation grid. C_{60} particles (Frontier Carbon Corporation, 99% purity) sublimated from an oven are deposited continuously on a substrate that is situated 23 cm downstream from the grid. The nitrogen ions arriving in front of the substrate are accelerated by the difference between a substrate bias voltage V_{sub} and a plasma potential ϕ_p, and irradiated to a C_{60} thin film throughout the period of C_{60} deposition.[15] The substrate is maintained at low temperatures during plasma irradiation using a water-cooling system because $N@C_{60}$ is unstable at ambient temperatures higher than about 500 K.[16] The plasma density and electron temperature are measured using Langmuir probes around the bottom of the mirror configuration. Analyses of the C_{60} thin films are performed by electron spin resonance (ESR) and

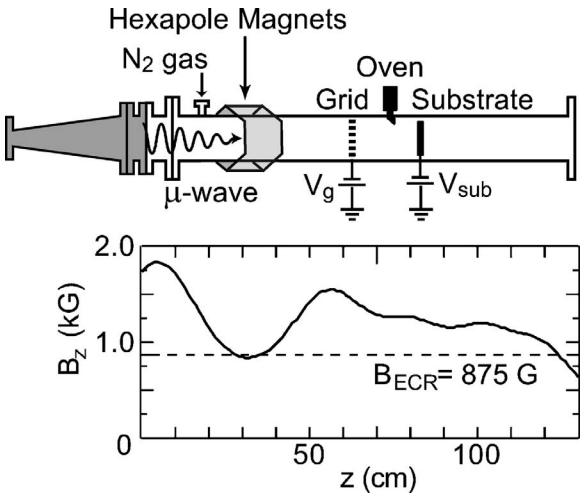

FIG. 1. Schematic diagram of experimental setup, together with the calculated axial profile of the magnetic field at the radial center.

UV absorption spectroscopy of high performance liquid chromatography (HPLC).

Figure 2 shows the (a) electron temperature T_e and (b) electron density n_e in the ECR region as a function of gas pressure P_{gas} of nitrogen in the cases of SM (open marks) and MM (closed marks) configurations. Although T_e gradually increases with a decrease in P_{gas} in the case of SM configuration, T_e saturates around $7\sim8$ eV for $P_{\mathrm{gas}} \leq 10^{-2}$ Pa and the generation of the plasma cannot be sustained for $P_{\mathrm{gas}} \leq 5\times10^{-3}$ Pa. In the case of the MM configuration, on the other hand, T_e increases drastically for $P_{\mathrm{gas}} \leq 3\times10^{-2}$ Pa and reaches around 30 eV at $P_{\mathrm{gas}} \simeq 5\times10^{-3} \sim 1\times10^{-2}$ Pa. This means that the electrons can effectively be heated by ECR in the MM configuration because confinement of electrons is improved by not only the axially but also radially increased magnetic fields realized by the hexapole magnets.

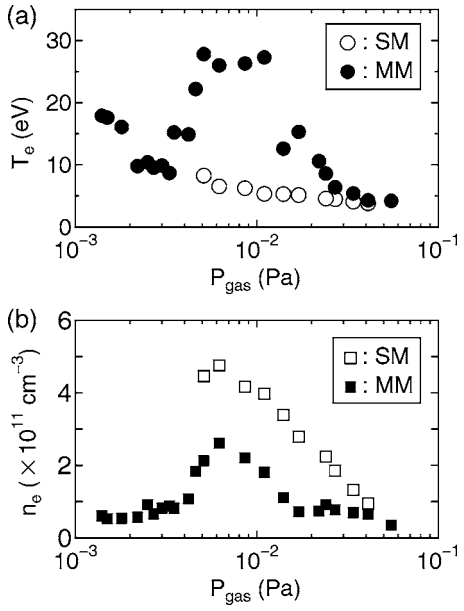

FIG. 2. (a) Electron temperature T_e and (b) electron density n_e in the ECR region as a function of gas pressure P_{gas} in the cases of the simple mirror (SM; open marks) and minimum-B mirror (MM; closed marks) configurations, where V_g and V_{sub} are electrically left floating.

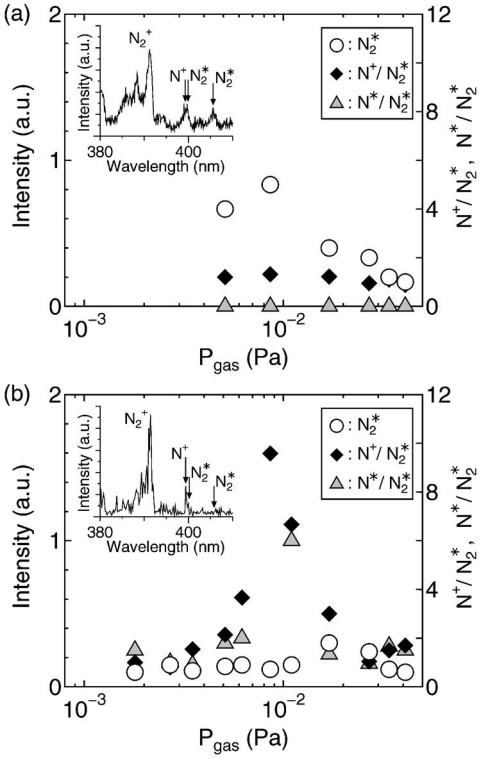

FIG. 3. Intensities of optical emission spectra as a function of gas pressure P_{gas} in the cases of (a) SM and (b) MM configurations, where V_g and V_{sub} are electrically left floating. The emission intensities of N_2^* (405.9 nm) are plotted referring to the left axis. On the other hand, the emission intensities of N^* (746.8 nm) and N^+ (399.5 nm) are normalized by that of N_2^* and plotted referring to the right axis. The inset shows the raw optical emission spectra for $P_{\mathrm{gas}}=8\times10^{-3}$ Pa.

The electron density n_e increases with a decrease in P_{gas} in both the cases of the SM and MM configurations until $P_{\mathrm{gas}} \simeq 6\times10^{-3}$ Pa. n_e in the MM configuration is slightly smaller than that in the SM configuration, which is caused by the change of the ECR area. Since the magnetic field in SM is almost uniform in the radial direction, the ECR point exists at the whole radial positions. In the case of the MM configuration, on the other hand, the ECR point is localized at some radial positions due to the radial gradient of the magnetic field, which cause the reduction of ECR area compared with the SM configuration and the resultant decrease in the density. However, the plasma cannot be generated for $P_{\mathrm{gas}} < 5\times10^{-3}$ Pa in the case of the SM configuration, while the plasma is stably sustained until 1×10^{-3} Pa in the MM configuration, which is attributed to the improvement of the electron confinement.

Figure 3 presents intensities of optical emission spectra as a function of nitrogen gas pressure P_{gas}, where the emission intensities of nitrogen-atom radical N^* (746.8 nm) and ion N^+ (399.5 nm) are normalized by that of nitrogen-molecule radical N_2^* (405.9 nm).[10] The intensity of N_2^* (open circles) gradually increases with a decrease in P_{gas} in the case of SM configuration [Fig. 3(a)], which corresponds to the change of n_e, as shown in Fig. 2(b). Although the inten-

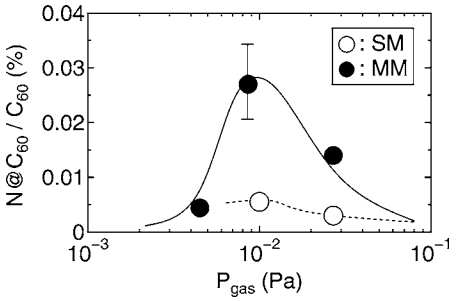

FIG. 4. Purity of $N@C_{60}$ as a function of gas pressure P_{gas} in the cases of the SM (open circles) and MM (closed circles) configurations, where $V_{sub}=-30$ V and V_g is adjusted to keep the amount of nitrogen ions flowing to the substrate constant. $N@C_{60}$ is synthesized several times under the condition of $P_{gas}=8\times10^{-3}$ Pa in the case of MM configuration, and consequently, the minimum and maximum purities are about 0.02 and 0.035%, respectively, and the average value is about 0.03% as shown by an error bar, evidencing the reproducibility of the increased purity of $N@C_{60}$.

sity of N^+ also increases with a decrease in P_{gas}, the intensity ratio of N^+ to N_2^* (closed diamonds) is almost constant. Therefore, it is found that dissociation degree of N_2^* is not changed by the decrease in P_{gas} in the case of the SM configuration.

On the other hand, dependence of the N_2^* intensity on P_{gas} in the MM configuration [Fig. 3(b)] is different from that in the SM configuration, i.e., the intensity of N_2^* suddenly decreases for $P_{gas}<1.5\times10^{-2}$ Pa. At this gas pressure, the intensities of N^* and N^+ are observed to increase, and as a result, the intensity ratio of N^* (gray triangles) and N^+ (closed diamonds) to N_2^* increases drastically around $P_{gas}\simeq8\times10^{-3}$ Pa. This highly dissociated nitrogen plasma is believed to be realized by the high-energy electrons because the intensity-ratio dependence corresponds to the electron-temperature dependence, which is shown in Fig. 2(a). Since the dissociation/ionization energy of nitrogen molecules is 25.4 eV, only a small number of the high-energy tail component of electrons can cause the ionization in the SM configuration, while the bulk component of the electrons which have the temperature of 30 eV can contribute to the dissociation/ionization in the MM configuration. Therefore, a large amount of N^* and N^+ can be produced in the MM configuration.

The nitrogen endohedral fullerene is yielded by irradiating C_{60} with the above-mentioned highly dissociated nitrogen plasma. C_{60} after plasma irradiation is dissolved in toluene and analyzed by ESR and HPLC for the purpose of estimating the concentration of $N@C_{60}$ and C_{60} in the solution, respectively,[11] and calculating the purity of $N@C_{60}$ ($N@C_{60}/C_{60}$: concentration of $N@C_{60}$ divided by that of C_{60}). Figure 4 shows the purity of $N@C_{60}$ as a function of gas pressure P_{gas} in the cases of the SM (open circles) and MM (closed circles) configurations, where $V_{sub}=-30$ V and V_g is adjusted to keep the amount of nitrogen ions flowing to the substrate constant. The purity is increased up to 0.03% at $P_{gas}\simeq8\times10^{-3}$ Pa in the MM configuration, which is one order of magnitude larger than that in the conventional SM configuration. The dependence of purity on P_{gas} is found to correspond to that of N^* and N^+ intensities (see Fig. 3). Therefore, it is concluded that the N^* and N^+ in the nitrogen plasma play a significant role in the synthesis of the nitrogen endohedral fullerene.

In summary, the ECR plasma source with minimum-B mirror configuration is found to generate the high-energy electrons, which leads to the effective production of the nitrogen-atom radicals and ions. This highly dissociated nitrogen plasma can efficiently yield the nitrogen endohedral fullerene.

The authors are indebted to Dr. T. Hirata for his collaboration in the preliminary measurements. This work was partly carried out at the Evaluation and Analysis Center, Research Institute of Electrical Communication, Tohoku University.

This work was supported by Japan Science and Technology Agency, Innovation Plaza Miyagi, and by a Grant-in-Aid for Scientific Research from the Ministry of Education, Culture, Sports, Science and Technology, Japan.

[1] W. Harneit, Phys. Rev. A **65**, 032322 (2002).
[2] T. Almeida Murphy, T. Pawlik, A. Weidinger, M. Höhne, R. Alcala, and J.-M. Spaeth, Phys. Rev. Lett. **77**, 1075 (1996).
[3] B. Pietzak, M. Waiblinger, T. Almeida Murphy, A. Weidinger, M. Höhne, E. Dietel, and A. Hirsch, Chem. Phys. Lett. **279**, 259 (1997).
[4] A. Weidinger, M. Waiblinger, B. Pietzak, and T. Almeida Murphy, Appl. Phys. A: Mater. Sci. Process. **66**, 287 (1998).
[5] H. Huang, M. Ata, and M. Ramm, Chem. Commun. (Cambridge) **2002**, 2076 (2002).
[6] M. Ata, H. Huang, and T. Akasaka, J. Phys. Chem. B **108**, 4640 (2004).
[7] T. Suetsuna, N. Dragoe, W. Harneit, A. Weidinger, H. Shimotani, S. Ito, H. Takagi, and K. Kitazawa, Chem.-Eur. J. **8**, 5079 (2002).
[8] P. Jakes, K.-P. Dinse, C. Meyer, W. Harneit, and A. Weidinger, Phys. Chem. Chem. Phys. **5**, 4080 (2003).
[9] M. Kanai, K. Porfyrakis, G. A. D. Briggs and T. J. S. Dennis, Chem. Commun. (Cambridge) **2004**, 210 (2004).
[10] A. Qayyum, S. Zab, S. Ali, A. Waheed, and M. Zakaullah, Plasma Chem. Plasma Process. **25**, 551 (2005).
[11] S. Abe, G. Sato, T. Kaneko, T. Hirata, R. Hatakeyama, K. Yokoo, S. Ono, K. Omote, and Y. Kasama, Jpn. J. Appl. Phys., Part 1 **45**, 8340 (2006).
[12] T. Kurita, M. Imanaka, M. Tsukada, T. Nakagawa, M. Kidera, I. Arai, and S.-M. Lee, Nucl. Instrum. Methods Phys. Res. B **192**, 429 (2002).
[13] G. S. Taki, D. K. Chakraborty, and R. K. Bhandari, Pramana, J. Phys. **59**, 775 (2002).
[14] S. Biri, A. Valek, L. Kenez, A. Janossy, and A. Kitagawa, Rev. Sci. Instrum. **73**, 881 (2002).
[15] T. Hirata, R. Hatakeyama, T. Mieno, and N. Sato, J. Vac. Sci. Technol. A **14**, 615 (1996).
[16] M. Waiblinger, K. Lips, W. Harneit, and A. Weidinger, Phys. Rev. B **64**, 159901 (2001).